Environ Sci Pollut Res (2017) 24:20446–20458
DOI 10.1007/s11356-017-9692-z

RESEARCH ARTICLE

Adsorption of As(III) versus As(V) from aqueous solutions by cerium-loaded volcanic rocks

Tsegaye Girma Asere[1] · **Kim Verbeken**[2] · **Dejene A. Tessema**[3] · **Fekadu Fufa**[4] · **Christian V. Stevens**[5] · **Gijs Du Laing**[1]

Received: 1 March 2017 / Accepted: 30 June 2017 / Published online: 14 July 2017

Abstract Contamination of drinking water with arsenic causes severe health problems in various world regions. Arsenic exists predominantly as As(III) and As(V) depending on the prevailing redox conditions of the environment. Most of the techniques developed for treating As(V) are not very effective for As(III), which is more toxic and mobile than As(V). In this study, novel cerium-loaded pumice (Ce-Pu) and red scoria (Ce-Rs) adsorbents were developed to remove both As(III) and As(V) ions from water. The Ce-Pu and Ce-Rs adsorbents were characterized using ICP-OES, EDX, and SEM. The experimental equilibrium sorption data fitted well Freundlich and Dubinin-Radushkevich (D-R) isotherms. The adsorption was very fast and reached an equilibrium within 2 h. Both Ce-Rs and Ce-Pu showed high As(III) and As(V) removal efficiency in a wide pH range between 3 and 9, which is an important asset for practical applications. The Ce-Pu and Ce-Rs adsorbents can be recycled and used up to three adsorption cycles without significant loss of their original efficiency. Accordingly, Ce-Pu and Ce-Rs seem to be suitable for removal of arsenic from aqueous systems.

Keywords Cerium · Arsenic · Adsorption · Red scoria · Pumice

Responsible editor: Guilherme L. Dotto

✉ Tsegaye Girma Asere
TsegayeGirma.Asere@UGent.be; tsegaye96@gmail.com

[1] Laboratory of Analytical Chemistry and Applied Ecochemistry, Ghent University (UGent), Coupure Links 653, 9000 Ghent, Belgium

[2] Department of Materials Science and Engineering, Ghent University (UGent), Technologiepark 903, 9052 Zwijnaarde, Belgium

[3] Southern Nations, Nationalities and Peoples' Region, Welkite University, Welkite, Ethiopia

[4] Department of Water Resources and Environmental Engineering, Jimma University, P.O. Box 378, Jimma, Ethiopia

[5] Department of Sustainable Organic Chemistry and Technology, Ghent University, Campus Coupure, Coupure Links 653, 9000 Ghent, Belgium

Introduction

Water is an essential component for life; however, clean potable water becomes scarce in the world. About 748 million people do not have access to safe water resources (Jadhav et al. 2015). Arsenic is a natural constituent of the earth's crust which affects millions of people around the world (Xie et al. 2016). Arsenic toxicity has already been known a long time in human civilization (Bolt 2012); however, arsenic-contaminated potable water was recognized as a global public health problem not longer than three decades ago (Fox et al. 2016). The primary exposure of the human body to arsenic is through the consumption of contaminated water, which leads to arsenic poisoning or arsenicosis (Rijith et al. 2016). Long-term exposure to arsenic-polluted water creates chronic health problems such as hyperkeratosis, skin lesions, black foot diseases, and bladder, lung, skin, kidney, and liver cancer (Chen et al. 1992; Chiou et al. 1995; Guzman et al. 2016). Accordingly, the World Health Organization (WHO) has set 0.01 mg/L as the maximum permissible level for total arsenic in drinking water (WHO 2006).

The presence of arsenic in the environment arises from both natural and anthropogenic sources. Weathering of arsenic-containing rocks is the major source of arsenic in groundwater. However, industrial waste discharges and application of arsenic-bearing herbicides and pesticides such as sodium arsenate, dimethylarsinic acid, monosodium

methanearsonate, and disodium methanearsonate also contribute significantly to the high arsenic concentration in the environment (Yazdani et al. 2016). Arsenic can exist in −3, 0, +3, and +5 oxidation states. However, the predominant arsenic species in natural water are the oxidation states of +3 and +5 depending on the prevailing redox conditions (Singh and Pant 2004). Under reducing conditions, As(III) is found, primarily as H_3AsO_3, $H_2AsO_3^-$, $HAsO_3^{2-}$, and AsO_3^{3-}, whereas As(V) can exist as H_3AsO_4, $H_2AsO_4^-$, $HAsO_4^{2-}$, and AsO_4^{3-} in oxidizing environments (Singh and Pant 2004). As(III) is much more mobile in natural water and is more toxic than As(V) (Kitchin and Wallace 2005; Styblo et al. 2000). At a pH below 9, the As(III) exists mainly in the molecular form H_3AsO_3, which is hard to remove by simple coagulation/precipitation or adsorption (Xie et al. 2016).

A number of arsenic removal technologies have been developed like oxidation, phytoremediation, coagulation–flocculation, ion-exchange, electrochemical and membrane technologies, and combinations thereof. Among them, adsorption has attracted much attention due to its easy operation and handling with no need for addition of chemicals, high removal efficiency, and low cost, not requiring large adsorbent volumes and not producing harmful by-products (Sanchez-Cantu et al. 2016; Singh et al. 2015). Adsorption is especially suitable for treating lower concentrations of pollutants and has often been suggested as a polishing step in the treatment process (Genz et al. 2004; Kumar et al. 2016). Various natural adsorptive materials have already been tested for the sorption of arsenic from water (Elizalde-Gonzalez et al. 2001; Elson et al. 1980; Rouff et al. 2016; Yazdani et al. 2016). They are considered as cost-effective for the remediation of arsenic pollution, particularly, in the low-income countries. However, the practical applicability of these natural adsorbents is limited either due to low efficiency, the need for pH adjustment, or dissolution problems (Fufa et al. 2014). Hence, different modifications such as coating natural materials with inorganic chemicals have been adopted. For instance, coating pumice with aluminum showed enhanced removal of arsenate (Asere et al. 2017; Heidari et al. 2011) from drinking water. Aluminum-coated zeolite showed a higher As(V) efficiency than aluminum-coated pumice (Rijith et al. 2016). Coating cement with iron oxide was used to treat both As(III) and As(V) (Kundu and Gupta 2006).

Many adsorbents containing rare earth elements, such as lanthanum compounds (Tokunaga et al. 1997), Ce(IV)-doped iron oxide adsorbent (Zhang et al. 2003), granular iron-cerium oxide (Zhang et al. 2010), nanostructured Fe(III)–Ce(IV) mixed oxide (Basu and Ghosh 2013), Ce-doped TiO_2 adsorbents (Li et al. 2011), hydrous cerium oxide nanoparticles (Li et al. 2012), cerium-loaded chitosan-polyvinyl alcohol composite (Sharma et al. 2014), orange waste loaded with lanthanum(III) and/or cerium(III) (Biswas et al. 2008), and cerium-exchanged zeolite (Haron et al. 2008b), have been employed for selective adsorption of arsenic. However, cerium-loaded volcanic rocks have not yet been tested previously to treat arsenic-contaminated water. Pumice and red scoria are available in many countries such as Italy, Turkey, Spain, Ethiopia, and Kenya (Alemayehu and Lennartz 2009). Hence, in this study, cerium-loaded pumice and red scoria were prepared for the first time and their As(III) and As(V) adsorption capacities were tested under varying conditions such as pH, adsorbent doses, and in the presence of commonly co-existing anions in aqueous systems.

Materials and methods

Adsorbent preparation

Volcanic rocks

The volcanic rocks (red scoria and pumice) were collected from volcanic cones of the Main Rift Valley, Ethiopia. The collected rock samples were washed repeatedly with deionized water and dried at 55 °C for 48 h (Far et al. 2012). Then, the dried adsorbents were crushed in a mortar and sieved into four size fractions as described in (Alemayehu and Lennartz 2009; Liu and Evett 2003). A fine particle size (0.075–0.425 mm) was used for coating with cerium (Asere et al. 2017).

Loading of cerium onto volcanic rocks

Loading of cerium onto volcanic rocks was carried out using 0.1, 0.25, or 0.5 M $Ce(NO_3)_3.6H_2O$. An adequate amount of $Ce(NO_3)_3.6H_2O$ solution was added to completely soak pumice and red scoria, separately, in Erlenmeyer flasks. The mixtures were shaken in an orbital shaker for 12 h at 200 rpm. The volcanic rocks were decanted, dried in an oven at 70 °C for 12 h, and soaked in 5 M NH_4OH. Then, the cerium-loaded volcanic rocks were decanted and dried in an oven at 70 °C. The cerium-loaded samples were washed several times with deionized water, dried at 70 °C for 48 h, and stored for subsequent use.

Adsorbent characterization

Chemical composition

All characterizations were performed for nontreated volcanic rocks as well as volcanic rocks treated with 0.25 M $Ce(NO_3)_3.6H_2O$. The elemental and oxide compositions of the adsorbents were analyzed using inductively coupled plasma–optical emission spectrometry (ICP-OES; Varian Vista-MPX CCD Simultaneous ICP-OES) and energy dispersive X-ray spectroscopy (EDX), respectively. The surface

morphology was studied using scanning electron microscope (FEG SEM JSM-7600F, JEOL, USA). The Brunauer–Emmett–Teller (BET) specific surface area of the adsorbents was determined from N_2 gas adsorption/desorption isotherms obtained using BEL, Japan, Inc. Belsorp mini-II.

pH and point of zero charge

The pH of the natural and Ce-coated volcanic rocks was measured using a pH meter in a 1:10 adsorbent/water ratio according to the standard method (Appel et al. 2003; Fufa et al. 2013). The point of zero charge (pH_{PZC}) of the adsorbents was determined following a standard method using 0.01 and 0.1 M solutions of NaCl as electrolyte and adding 0.1 M solutions of NaOH or HCl (Asere et al. 2017; Karimaian et al. 2013; Sepehr et al. 2013).

Porosity

Porosity is a measure of the void spaces in a material, and is a measure of the volume of voids over the total volume. The porosity of pumice and red scoria was determined following the methods described in Sekomo et al. (2012).

Chemicals and reagents

All glassware and bottles were washed using 1% HNO_3 and rinsed with deionized water before use. Stock solutions of 1000 mg/L As(V) and 1000 mg/L As(III) were prepared by dissolving an appropriate amount of $Na_2HAsO_4.7H_2O$ and $NaAsO_2$ (Merck KGaA, Darmstadt, Germany), separately, in deionized water and stored in the refrigerator at 4 °C. Synthetic aqueous As(III) and As(V) solutions for the adsorption experiments were prepared by diluting the stock solutions with deionized water to obtain a concentration of As(III) and As(V), separately, in the range of 0.1–25 mg/L. Solutions of bicarbonate, chloride, nitrate, sulfate, and phosphate anions were prepared from their respective sodium salts.

Batch As(III) and As(V) adsorption studies

Batch adsorption experiments were performed to evaluate the adsorption of As(III) or As(V) on Ce-Pu and Ce-Rs in aqueous solution. All adsorption/desorption experiments were carried out using Pu and Rs treated with 0.25 M $Ce(NO_3)_3$, except 0.1 or 0.5 M $Ce(NO_3)_3.6H_2O$-treated Pu and Rs in preliminary testing experiments. The experiments were performed in triplicate using 50-mL polyethylene plastic centrifuge tubes. The required quantity of Ce-Rs or Ce-Pu adsorbent was added to 25 mL of As(III) or As(V) solution, and the pH was adjusted using 0.1 M NaOH or 0.1 M HCl. The closed tubes were kept on a horizontal shaker at 200 rpm for a predetermined period of time at 24 ± 1 °C. Then, the aqueous phase was filtered through a 0.45-μm regenerated cellulose disposable syringe filter (MACHERY-NAGEL GmbH & Co., KG, Germany) and the residual arsenic in the filtrate was measured using ICP-MS (ELAN DRC-e, PerkinElmer).

The arsenic adsorption capacity, q_t (mg/g), at time t (min), and the arsenic removal efficiency (% adsorption) were determined using Eqs. (1) and (2), respectively.

$$q_t = (C_0 - C_t)\left(\frac{V}{W}\right) \quad (1)$$

$$Adsorption(\%) = \left(\frac{C_0 - C_t}{C_0}\right) \times 100 \quad (2)$$

where C_0 and C_t (mg/L) are the initial arsenic concentration and the concentration at time t (min), respectively; V (L) is the solution volume; and W (g) is the adsorbent mass.

The effects of pH on As(III) and As(V) adsorption were studied in solutions with initial As(III) or As(V) concentrations of 0.25 mg/L in the pH range of 3–12. The adsorption kinetics were studied for the contact times ranging from 0 to 540 min at optimum pH. Then, the adsorption isotherms were constructed at the optimum pH and contact time for As(III) or As(V) with initial concentrations ranging from 0.25 to 25 mg/L. The effect of competing ions (5–500 mg/L of Cl^-, NO_3^-, HCO_3^-, SO_4^{2-}, and PO_4^{3-}) (Fufa et al. 2014) was evaluated in the 0.25 mg/L solution of As(III) or As(V) at optimum condition.

Results and discussion

Adsorbent characterization

Chemical composition

The elemental composition of the adsorbents was determined by ICP-OES and further confirmed by EDX. The adsorbents were mainly composed of the element silicon. Elements such as Al, Fe, K, and Ca are also found in large proportions. The other elements are present in relatively smaller amounts (Table 1). Silicon dioxide (SiO_2) was the major oxide that composes the adsorbents as evidenced by the EDX measurement. Similar values were reported by Alemayehu and Lennartz (2009) for red scoria and pumice. Absence of hazardous substances in the adsorbents suggested that the cerium-loaded pumice and red scoria are appropriate to treat arsenic-contaminated water.

The average amount of cerium loaded onto the pumice and red scoria particles was 51.9 and 10.2 mg Ce/g, respectively. The EDX measurement indicated that 11.1 and 8.4% cerium oxide was loaded on pumice and red scoria, respectively. The greater amount of cerium oxide loaded on pumice than red scoria is due to pumice being more porous than red scoria. The

Table 1 Elemental and oxide composition of pumice (Pu), red scoria (Rs), Ce-Pu, and Ce-Rs

Element	Pu % (wt)	RS % (wt)	Ce-Pu % (wt)	Ce-Rs % (wt)	Oxide	Pu %	Rs %	Ce-Pu %	Ce-Rs %
Si	27.2	18.4	26.6	19.4	SiO_2	68.7	44.5	62.0	41.5
Al	5.4	10.4	5.7	10.4	Al_2O_3	11.9	18.2	10.8	19.5
Fe	3.1	7.2	3.0	7.4	FeO	6.9	14.3	5.6	10.9
K	4	0.4	3.7	0.4	K_2O	6.6	0.6	4.8	0.4
Ca	0.4	9.5	0.4	9.3	CaO	0.9	11.3	–	10.9
Na	1.1	2.1	1.0	2.0	Na_2O	–	3.5	1.5	3.0
Mn	0.1	0.1	0.1	0.1	MnO	0.3	0.3	0.3	–
Mg	0.1	3.1	0.1	3.0	MgO	0.2	4.9	–	3.5
Zn	<0.1	<0.1	<0.1	<0.1	ZnO	1.1	–	–	–
Ce	<0.1	<0.1	5.2	1.0	TiO_2	0.2	2.4	–	1.9
Cr	<0.1	<0.1	<0.1	<0.1	SO_3	0.1	–	–	–
Cu	<0.1	<0.1	<0.1	<0.1	CuO	1.7	–	1.7	–
Co	<0.1	<0.1	<0.1	<0.1	NiO	1.3	–	2.3	–
Cd	<0.1	<0.1	<0.1	<0.1	Ce_2O_3	–	–	11.1	8.4
Ni	<0.1	<0.1	<0.1	<0.1					
Pb	<0.1	<0.1	<0.1	<0.1					
As	<0.1	<0.1	<0.1	<0.1					

porosity of pumice (76.6%) was found to be much higher than red scoria (44.7%). The porosity of pumice can reach up to 90% (Asgari et al. 2012; Kitis et al. 2007). Alemayehu and Lennartz (2009) also mentioned the existence of a continuum (skeletal structure) pore space in pumice while the pore space of red scoria is dominated by dead-end pores. The SEM image (Fig. 1) also shows the difference in morphology between red scoria and pumice. Coating with cerium improved the specific surface area of pumice from 2.82 to 14.49 m^2/g but for red scoria only from 1.49 to 3.20 m^2/g.

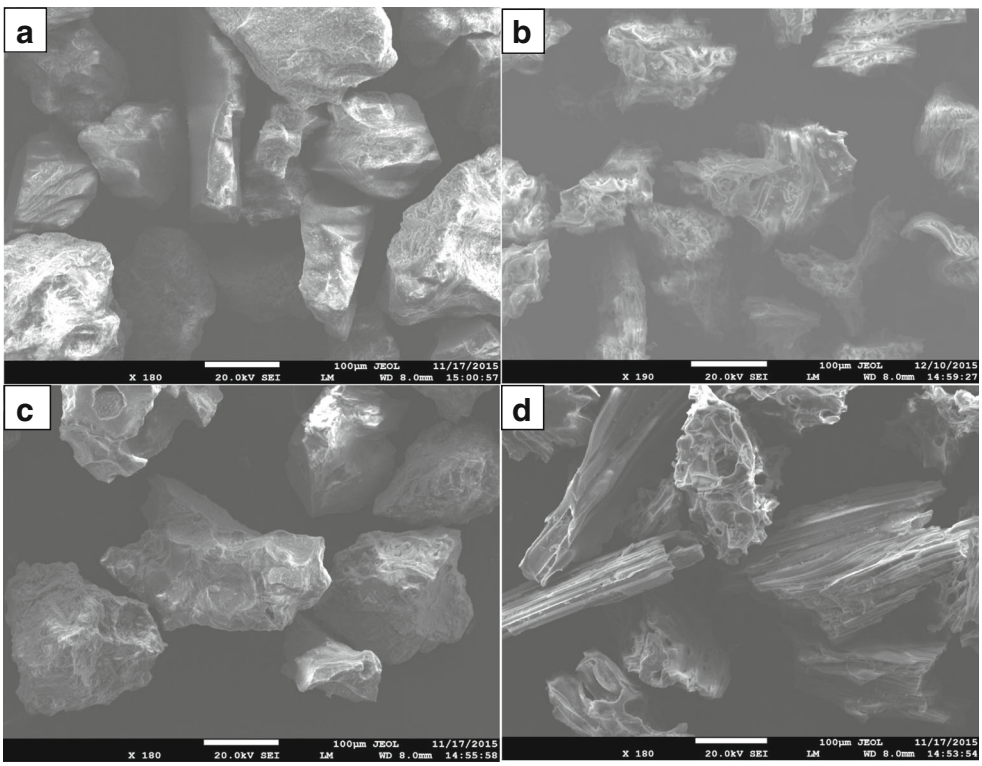

Fig. 1 SEM image of red scoria and pumice (fine particle size). **a** Rs, **b** Pu, **c** Ce-Rs, and **d** Ce-Pu

Adsorption of As(III) or As(V) on Ce-Pu and Ce-Rs

Preliminary study

Preliminary studies were conducted using 0.1, 0.25, and 0.5 M $Ce(NO_3)_3$-treated volcanic rocks at the dose of 8 g/L of Ce-Rs or 5 g/L of Ce-Pu. Each adsorbent was mixed with 25 mL of 0.25 mg/L As(V) solution and then shaken for 24 h at pH ~7.0. When the $Ce(NO_3)_3$ concentration increased from 0.1 to 0.25 M, Ce-Pu showed a small change in As(V) removal (99.29 to 99.95%) for 0.25 mg/L initial As(V) and from 98.12 to 99.66% for 1.0 mg/L initial As(V). For Ce-Rs, as the concentration of $Ce(NO_3)_3$ increased from 0.1 to 0.25 M, the As(V) removal efficiency also increased from 99.37 to 99.75% for 0.25 mg/L initial As(V) and from 86.77 to 89.11% for 1.0 mg/L initial As(V). However, with further increase in concentration of $Ce(NO_3)_3$ to 0.5 M, both Ce-Pu and Ce-Rs showed negligible change. Therefore, 0.25 M $Ce(NO_3)_3$ was chosen to prepare Ce-loaded volcanic rocks and used in all experiments.

Batch adsorption

The preliminary study indicated that 0.25 M $Ce(NO_3)_3.6H_2O$ was an optimum concentration to prepare cerium-loaded red scoria and pumice. The adsorption of As(III) or As(V) onto the Ce-loaded pumice and red scoria were found to be time dependent at different initial arsenic concentrations. The arsenic removal efficiency of Ce-loaded volcanic rocks decreased as the initial As(III) or As(V) concentration increased from 0.25 to 2.0 mg/L (Fig. 2). This is due to As(III) or As(V) interacting easily with the binding sites at low initial concentration, while only part of As(III) or As(V) combined with the finite binding sites at high initial concentrations (Liu et al. 2013). For the 0.25 mg/L initial As(III) concentration, the adsorption percentage increased from 79.5 to 97.1% (Ce-Pu) and from 72.9 to 95.5% (Ce-Rs), whereas for As(V), the adsorption percentage increased from 89.4 to 99.1% (Ce-Pu) and from 70.1 to 98.5% (Ce-Rs) with an increase in agitation time (5–30 min). Thereafter, it increased gradually until equilibrium (Fig. 2a). The results revealed that As(III) and As(V) adsorption was fast in the early stage of contact, i.e., during the first 15 min, and then slowed down near the equilibrium. The rapid adsorption at the initial stage could be due to availability of a lot of adsorption sites and smaller mass transfer resistance in the pores (Liu et al. 2013). The next gradual adsorption stage may involve intraparticle diffusion which controls the adsorption rate up to the equilibrium point. At equilibrium, the amount of As(III) adsorbed onto Ce-Rs and Ce-Pu adsorbents were 0.029 mg/g (99.0%) and 0.047 mg/g (99.3%), respectively. On the other hand, As(V) adsorbed onto Ce-Rs and Ce-Pu adsorbents at equilibrium were 0.033 mg/g (99.6%) and 0.051 mg/g (99.7%), respectively.

Kinetics

Pseudo-first-order and pseudo-second-order models were used to analyze adsorption kinetics data to investigate the adsorption mechanism. The nonlinear expressions of the pseudo-first-order and pseudo-second-order models (Kumar 2006) are given in Eqs. (3) and (4), respectively.

$$q_t = q_e\left(1-\exp^{-K_1 t}\right) \tag{3}$$

$$q_t = \frac{K_2 q_e^2 t}{1 + K_2 q_e t} \tag{4}$$

where k_1 (min^{-1}) is the pseudo-first-order rate constant, k_2 (g mg^{-1} min^{-1}) is the pseudo-second-order rate constant, and q_t and q_e are the As(III) or As(V) adsorption capacities (mg/g) at any time t (min) and at equilibrium, respectively. The nonlinear plots of the pseudo-first-order and pseudo-second-order arsenic adsorption kinetics are given in Fig. 3a, b, and the values of k_1, k_2, $q_{e,cal}$ (calculated), and $q_{e,exp}$ (experimental) are also presented in Table 2.

The analysis of the kinetic data of As(III) and As(V) removal showed that the values of $q_{e,cal}$ and $q_{e,exp}$ were similar for each adsorbent. At low concentration (0.25 mg/L), R^2 values of the pseudo-first-order kinetic model were high enough to explain the adsorption process of As(V) by Ce-loaded volcanic rocks (Table 2). However, at higher concentration (2.0 mg/L), the values of R^2 for the pseudo-first-order

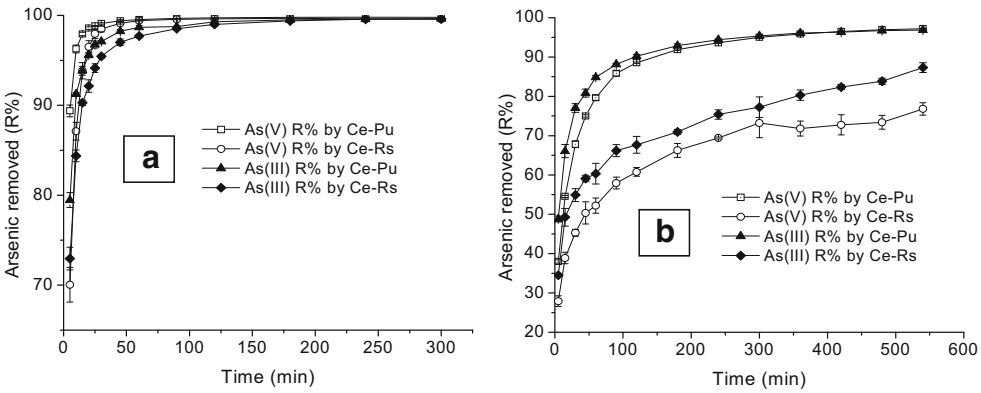

Fig. 2 Effect of contact time on removal of As(III) and As(V) by Ce-Pu (5-g/L dose) and Ce-Rs (8 g/L) at initial As(III) or As(V) concentration of **a** 0.25 mg/L and **b** 2.0 mg/L at pH 7, shaking at 200 rpm at 24 ± 1 °C

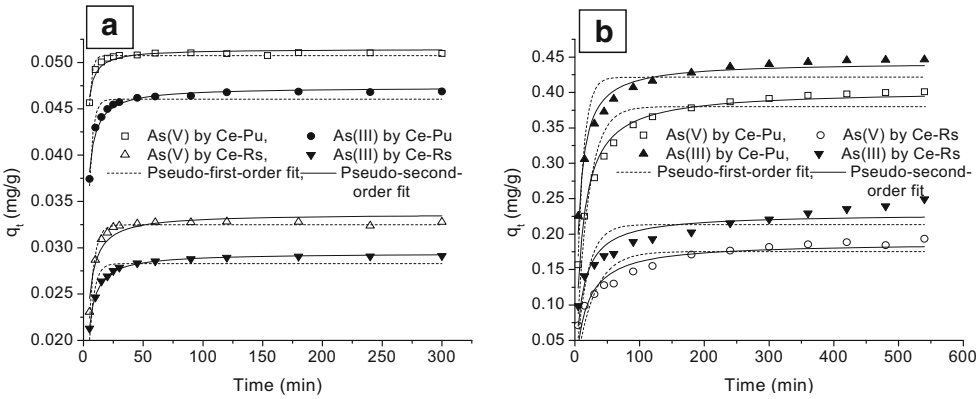

Fig. 3 Plots of kinetic models **a** 0.25 mg/L As(III) or As(V) and **b** 2.0 mg/L As(III) or As(V) at dose of 5 g/L (Ce-Pu) and 8 g/L (Ce-Rs) at pH 7, shaking at 200 rpm at 24 ± 1 °C

model were not satisfactory compared to the pseudo-second-order-kinetic model (R^2 = 0.97 (Ce-Pu) and 0.90 (Ce-Rs) for As(V) removal). On the other hand, the kinetics of As(III) removal was independent of concentration but better described by the pseudo-second-order model than the pseudo-first-order model. These observations are in good agreement with the pseudo-second-order model proposed by Li et al. (2012) for both As(III) and As(V) removal using hydrous cerium oxide nanoparticles.

The adsorption affinity ($V_0 = k_2 q_e^2$) provides information on the adsorption rate at the beginning of the adsorption process. The calculated values of k_2, $q_{e,\mathrm{cal}}$, and V_0 for both adsorbents showed a decrease in k_2 and V_0 values and an increase in the value of $q_{e,\mathrm{cal}}$ with the increase in the concentration of As(V) from 0.25 to 2.0 mg/L. However, for As(III), k_2 decreases while V_0 and $q_{e,\mathrm{cal}}$ values increase when the concentration of As(III) increases from 0.25 to 2.0 mg/L. These results indicate that as the arsenic concentration increases, the adsorption become slower for As(V) while faster for As(III). It is also clearly shown that at low arsenic concentration (0.25 mg/L) (Fig. 3), more As(V) was removed compared to As(III). However, when the initial arsenic concentration increased from 0.25 to 2 mg/L, more As(III) than As(V) was adsorbed. A higher As(III) sorption capacity than As(V) was also reported for 5 g/L initial arsenic concentration by Gupta and Ghosh (2009). This may be due to a difference in the mechanisms involved in the adsorption of As(III) and As(V) onto the adsorbents.

The adsorption kinetics were also examined by applying the Weber and Morris intraparticle diffusion model (Fufa et al. 2014; Viswanathan et al. 2009) as given by Eq. (5).

$$q_t = k_p t^{0.5} + c \tag{5}$$

where k_p (mg/(g min$^{0.5}$) is the intraparticle diffusion rate constant, time t (min), and c (mg/g) is the intercept of the intraparticle diffusion model.

It is clear that each curve shows a multi-linear plot (Fig. 4). However, each curve does not pass through the origin which

Table 2 Parameters of the pseudo-first-order and pseudo-second order kinetic models for As(III) and As(V) adsorption on Ce-Pu and Ce-Rs

Parameter	As(V) by Ce-Pu				As(III) by Ce-Pu			
	Pseudo-first-order		Pseudo-second-order		Pseudo-first-order		Pseudo-second-order	
C_0 (mg/L)	0.25	2.0	0.25	2.0	0.25	2.0	0.25	2.0
$q_{e,\mathrm{exp}}$ (mg/g)	0.051	0.39	0.051	0.39	0.047	0.44	0.047	0.44
$q_{e,\mathrm{cal}}$ (mg/g)	0.051	0.38	0.051	0.40	0.046	0.42	0.047	0.44
k_1 (min^{-1})	0.45	0.05	–	–	0.32	0.10	–	–
k_2 (g/(mg min))	–	–	34.84	0.22	–	–	17.64	0.37
V_0 (mg/(g min))	–	–	0.091	0.035	–	–	0.039	0.072
R^2	0.922	0.847	0.937	0.974	0.887	0.763	0.977	0.965
Parameter	As(V) by Ce-Rs				As(III) by Ce-Rs			
	Pseudo-first-order		Pseudo-second-order		Pseudo-first-order		Pseudo-second-order	
C_0 (mg/L)	0.25	2.0	0.25	2.0	0.25	2.0	0.25	2.0
$q_{e,\mathrm{exp}}$ (mg/g)	0.033	0.19	0.033	0.19	0.029	0.23	0.029	0.23
$q_{e,\mathrm{cal}}$ (mg/g)	0.033	0.18	0.034	0.19	0.028	0.21	0.029	0.23
k_1 (min^{-1})	0.23	0.04	–	–	0.25	0.06	–	–
k_2 (g/(mg min))	–	–	15.98	0.32	–	–	18.11	0.39
V_0 (mg/(g min))	–	–	0.019	0.012	–	–	0.015	0.021
R^2	0.975	0.728	0.914	0.901	0.836	0.613	0.997	0.848

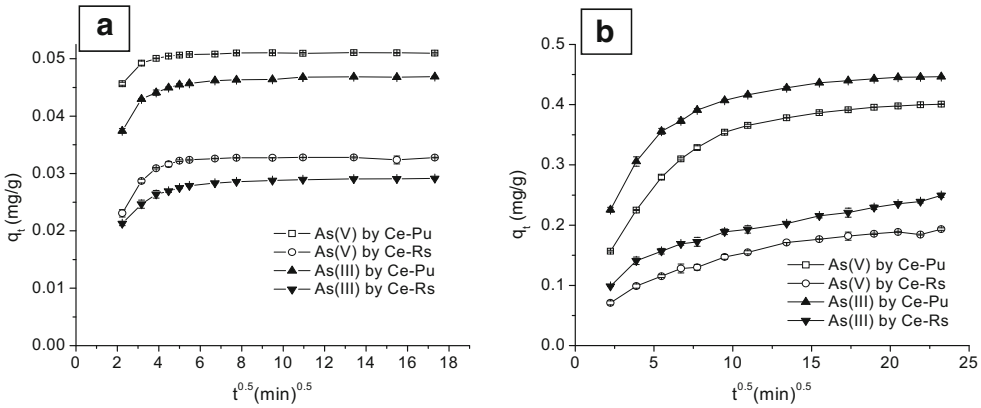

Fig. 4 Intraparticle diffusion plots of As(III) and As(V) adsorption on Ce-Pu and Ce-Rs. **a** 0.25 mg/L As(III) or As(V). **b** 2 mg/L As(III) or As(V)

indicates that intraparticle diffusion was not the only rate-determining step (Pillewan et al. 2014).

Effect of pH on As(III) versus As(V) removal

pH is one of the important factors which significantly influence the adsorption process. This is attributed to the pH dependence of the surface charge of the adsorbents and arsenic speciation in solution. As(V) occurs as $H_2AsO_4^-$ in the pH range of 3–6, and as $HAsO_4^{2-}$ at higher pH values (between pH 8 and 10.5). In the intermediate region (6–8), both species co-exist together (Basu and Ghosh 2013). On the contrary, As(III) exists predominantly as the neutral molecular form (H_3AsO_3) at a pH ≤9.2 (Wang et al. 2016).

Coating with cerium lowered the pH in water and the point of zero charge (pH_{PZC}) of pumice and red scoria. The pH in water of the adsorbents was 9.38 (red scoria), 7.84 (pumice), 6.88 (Ce-Rs), and 6.12 (Ce-Pu), respectively. The pH_{PZC} for red scoria and pumice was 7.5 and 6.8, respectively, whereas the pH_{PZC} of Ce-Rs and Ce-Pu was 7.04 and 5.38, respectively. Similar pH_{PZC} values were reported for natural pumice by Sepehr et al. (2014). Therefore, the surface charge of adsorbent is positive when the solution pH is below pH_{PZC} (Ce-Pu (5.38) and Ce-Rs (7.04)) and negative when the pH is above pH_{PZC} of the adsorbent. The variation in removal efficiency with respect to pH was investigated over a pH range of 3–12 and presented in Fig. 5a, b. Ce-Rs exhibited high removal of As(III) (>95%) and As(V) (>99%), whereas Ce-Pu could remove >99% of As(III) and As(V) in the pH range of 3–9. The Ce-Pu and Ce-Rs adsorbents showed a remarkable efficiency in a wide pH range compared to most other adsorbents such as iron- and manganese-coated pumice (Far et al. 2012), feldspars (Yazdani et al. 2016), and activated alumina (Singh and Pant 2004). Such unique performance of Ce-Pu and Ce-Rs adsorbents over a wide pH range (3–9) was previously rarely reported for the more mobile and toxic As(III). Moreover, for 0.25 mg/L initial arsenic concentration, the equilibrium arsenic concentration in the pH range of 3–9 was below the WHO permissible limits for arsenic in the drinking water (0.01 mg/L). Thus, a single step highly efficient As(III) and As(V) removal process is possible with Ce-Rs or Ce-Pu, which eliminates the requirement of pre-treatment (oxidation and pH adjustment).

The low leaching of the cerium from the cerium-loaded volcanic rocks, 0.01 up to 0.09 mg/L in the pH range of 4–9, reduces the risk of secondary pollution in the treatment process. The adsorption experiments were conducted at neutral pH for optimization of other adsorption parameters. The observed rapid decrease of As(V) uptake when the pH increases above 9 was in good agreement with previous reports on other cerium-based adsorbents (Biswas et al. 2008; Li et al. 2012, 2011). It could be due to Coulomb repulsion between

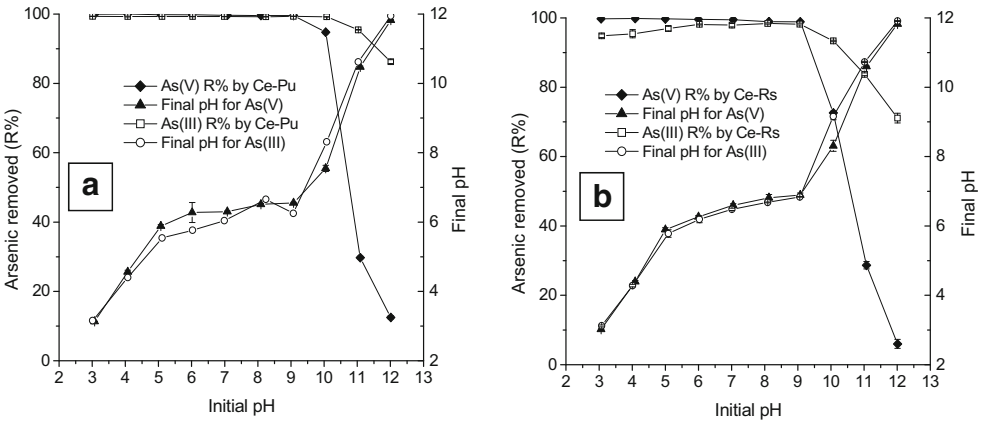

Fig. 5 Effect of initial pH on removal of As(III) and As(V) by **a** Ce-Pu (5-g/L dose) and **b** Ce-Rs (6-g/L dose): initial arsenic concentration 0.25 mg/L, shaking for 2 h at 200 rpm at 24 ± 1 °C

negatively charged adsorbent surfaces and arsenate ions and/or competition for active surface sites between arsenate ions and hydroxyl ions, both of which hinder arsenate and arsenite removal. However, compared with As(V), the As(III) adsorption onto Ce-Pu and Ce-Rs was just affected very slightly by the increase of solution pH above 9. This suggests that strong chemical attraction exists between As(III) anions and cerium(hydr)oxide and the adsorption energy was sufficient to overcome most of the repulsion effect from the increase of the solution pH (Li et al. 2012). Moreover, the high removal of As(III) in its uncharged form at a pH lower than pH_{PZC} of the adsorbents suggests that specific adsorption dominates in the adsorption of As(III) onto Ce-Rs and Ce-Pu adsorbents, whereas nonspecific adsorption (electrostatic ionic interaction) could be the main removal mechanism for As(V).

Effect of initial concentration

The percent removal of As(III) and As(V) decreased with the initial As(III) or As(V) concentration increasing from 0.25 to 25 mg/L (Fig. 6a, b). On the other hand, the adsorption capacity increased with increasing initial As(III) or As(V) concentration. This may be due to the availability of a higher amount of arsenic per unit mass of the adsorbents (Alemu et al. 2014). As the initial As(III) and As(V) concentration increased, more As(III) than As(V) was adsorbed per unit mass of Ce-Pu and Ce-Rs. It is also clearly shown that at low arsenic concentration (0.25 mg/L) (Fig. 3), more As(V) was removed compared to As(III). However, when the initial arsenic concentration increased from 0.25 to 2 mg/L, more As(III) than As(V) was adsorbed. A higher adsorption capacity for As(III) than As(V) was reported for various adsorbents (Gupta and Ghosh 2009; Li et al. 2012). The higher maximum adsorption capacity of As(III) compared to As(V) could be explained based on the surface charge of the adsorbents and speciation of As(III) and As(V) at initial pH (7.0) and equilibrium pH (5.9–6.7). As(V) occurs as $H_2AsO_4^-$ and $HAsO_4^{2-}$ at pH values between 6 and 8. The surface charge of Ce-Pu and Ce-Rs adsorbents is positive at pH <5.4 and pH<7, respectively. Hence, as the initial concentration of As(V) increases, the amount of $H_2AsO_4^-$ and $HAsO_4^{2-}$ ions in the boundary layer of the adsorbents surface increased and would tend to repel the $H_2AsO_4^-$ and $HAsO_4^{2-}$ ions in the aqueous solution. These electrostatic factors could influence both the kinetics and equilibrium of arsenate adsorption. Since As(III) species exist mainly as the neutral molecular form (H_3AsO_3) at a pH ≤9.2, they do not exhibit much repulsion between the adsorbed species and the As(III) in the aqueous solution. This is because As(III) occupies adsorption sites as $As(OH)_3$ with H-bonding (Basu and Ghosh 2013). As a result, the adsorption of As(III) increases more than As(V) with increasing initial concentration.

The Ce-Rs can lower about 0.25 mg/L of As(III) or As(V) to a concentration of arsenic below the threshold level recommended by WHO (<0.01 mg/L) for drinking water. Similarly, Ce-Pu can lower 0.50 mg/L of As(III) or 0.76 mg/L of As(V) to a concentration of arsenic below the WHO guideline. Therefore, it can be concluded that Ce-Rs and Ce-Pu are very promising absorbents for the treatment of both As(III) and As(V) from drinking water.

Adsorption isotherm

The amount of arsenic adsorbed per unit mass of Ce-Pu and Ce-Rs was correlated with the liquid-phase concentration at equilibrium using Langmuir, Freundlich, and D-R adsorption isotherms as given in Eqs. (6)–(9).

$$q_e = \frac{Q_{\max} b C_e}{(1 + bC_e)} \tag{6}$$

$$q_e = K_F C_e^{1/n} \tag{7}$$

$$q_e = q_m \exp\left(-K_{DR}\varepsilon^2\right) \tag{8}$$

$$\varepsilon = RTln\left(1 + 1/C_e\right) \tag{9}$$

where C_e (mg/L) is the concentration of As(III) or As(V) in the aqueous phase at equilibrium; $Q_{\max}$ (mg/g) is the maximum adsorption capacity based on the Langmuir equation; b (L/mg)

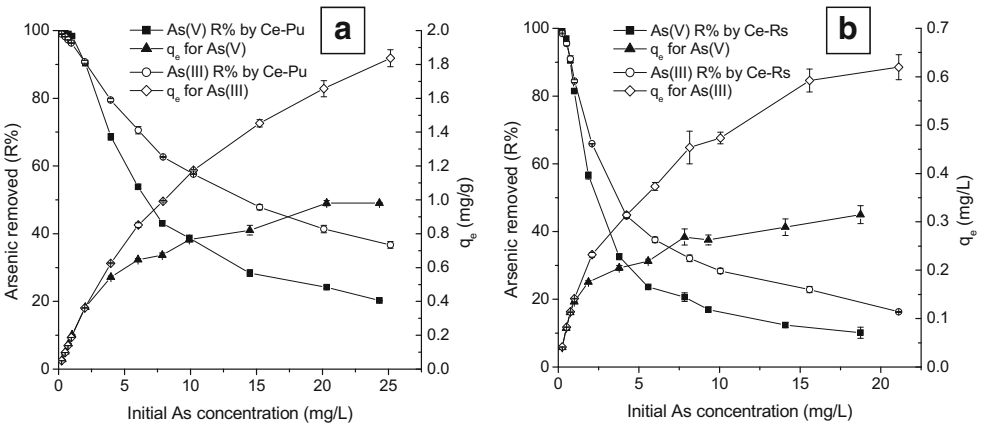

Fig. 6. Effect of initial concentration on removal of As(III) and As(V) by **a** Ce-Pu (5-g/L dose) and **b** Ce-Rs (6-g/L dose): initial pH 7, shaking for 2 h at 200 rpm at 24 ± 1 °C

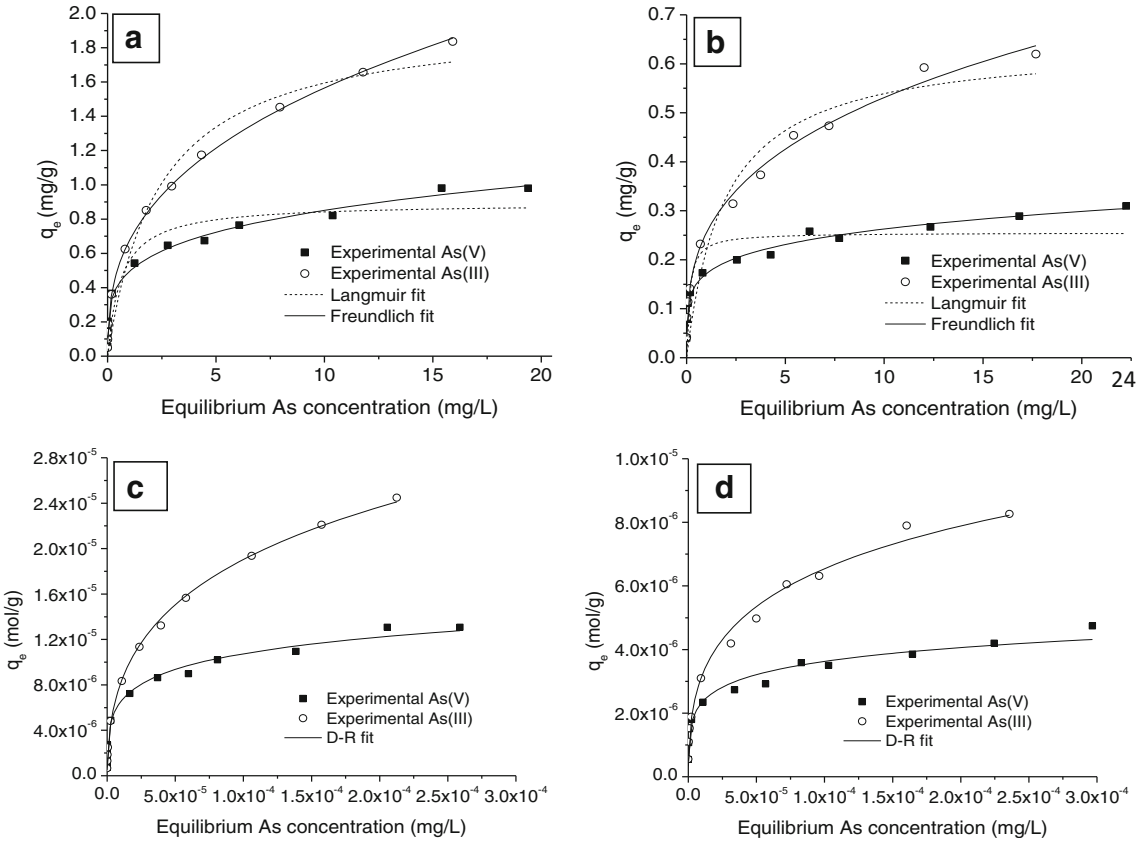

Fig. 7 Isotherm of equilibrium adsorption of As(III) and As(V) on Ce-Pu (**a**, **c**) and Ce-Rs (**b**, **d**)

is the Langmuir constant; K_F ($mg^{1-1/n}\,L^{1/n}/g$) is the adsorption coefficient based on the Freundlich equation; $1/n$ is the adsorption intensity based on the Freundlich equation; q_e (mol/g) and q_m (mol/g) are the equilibrium adsorption capacity and the theoretical monolayer saturation capacity, respectively, based on the D-R equation; K_{DR} (mol^2/kJ^2) is the activity coefficient related to the mean sorption energy; ε (mol^2/kJ^2) is the Polanyi potential; R (kJ/(mol K)) is the gas constant; and T (K) is the temperature of the equilibrium experiment. The isotherm plots of the equilibrium adsorption of As(III) and As(V) are graphically presented in Fig. 7a–d. The adsorption parameters evaluated from analysis of isotherm models were listed in Table 3.

Comparison of correlation coefficient (R^2) values for As(III) and As(V) removal by Ce-coated volcanic rocks indicates that both the Freundlich and D-R isotherm models fitted better to experimental data than the Langmuir model. The maximum sorption capacity of Ce-Pu and Ce-Rs adsorbents

Table 3 Isotherm parameters of the adsorption of As(III) and As(V) on Ce-Pu and Ce-Rs

Isotherm	Parameters	As(V) by Ce-Pu	As(III) by Ce-Pu	As(V) by Ce-Rs	As(III) by Ce-Rs
Langmuir	q_{max} (mg/g)	0.893	1.974	0.255	0.643
	b (L/mg)	1.64	0.419	7.131	0.518
	R_L	0.025–0.683	0.024–0.710	0.024–0.712	0.028–0.707
	R^2	0.879	0.963	0.8	0.903
Freundlich	K_F ($(mg^{1-1/n}\,L^{1/n})/g$)	0.494	0.672	0.172	0.255
	n	4.24	2.726	5.408	3.135
	R^2	0.992	0.999	0.986	0.994
D-R	q_m (mol/g)	2.60×10^{-5}	8.55×10^{-5}	7.93×10^{-6}	2.37×10^{-5}
	K_{DR} (mol^2/KJ^2)	1.7×10^{-3}	2.89×10^{-3}	1.5×10^{-3}	2.47×10^{-3}
	E_{DR} (KJ/mol)	17.2	13.2	18.3	14.2
	R^2	0.991	0.998	0.971	0.988

Table 4 Maximum adsorption capacity of Ce-Pu and Ce-Rs compared with other adsorbents

Adsorbents	pH	Dosage (g/L)	Q_{max} As(III) (mg/g)	Q_{max} As(V) (mg/g)	References
Ceria micro/nanocomposite	3	2		6.7	Zhong et al. (2007)
Feldspar	3	8		0.235	Yazdani et al. (2016)
Iron oxide-coated sand	7.5	20	0.286		Gupta et al. (2005)
Mn-substituted iron oxyhydroxide	7	2	4.58	5.72	Lakshmipathiraj et al. (2006)
Manganese oxide-coated zeolite	7	10		0.151	Massoudinejad et al. (2015)
Cerium-loaded cation exchange resin	5–6	5	2.597	2.384	He et al. (2012)
Cerium-exchanged zeolite P	6–7	7.5		8.72	Haron et al. (2008a)
Iron-oxide coated sands	7	24	0.012	0.021	Hsu et al. (2008)
Kaolinite		40		0.86	Mohapatra et al. (2007)
Ce-Rs	7	8	0.643	0.255	This study
Ce-Pu	7	5	1.974	0.893	This study

obtained from the Langmuir isotherm for As(III) and As(V), in this study, is comparable to some of the natural and modified adsorbents reported in previous work (Table 4).

In the Freundlich isotherm, the range of $1/n$ values between 0 and 1 also indicated that the adsorption is favorable (He et al. 2015). The D-R isotherm model assumes that adsorbates bind first with the energetically most favorable sites, after which multi-layer adsorption occurs (Peric et al. 2004). The mean sorption energy, E_{DR} (kJ/mol), of equilibrium As(III) and As(V) adsorption were computed from the D-R isotherm using the equation $E_{DR} = (2K_{DR})^{-0.5}$ (Gupta and Ghosh 2009). The K_{DR} provides information about the mean free

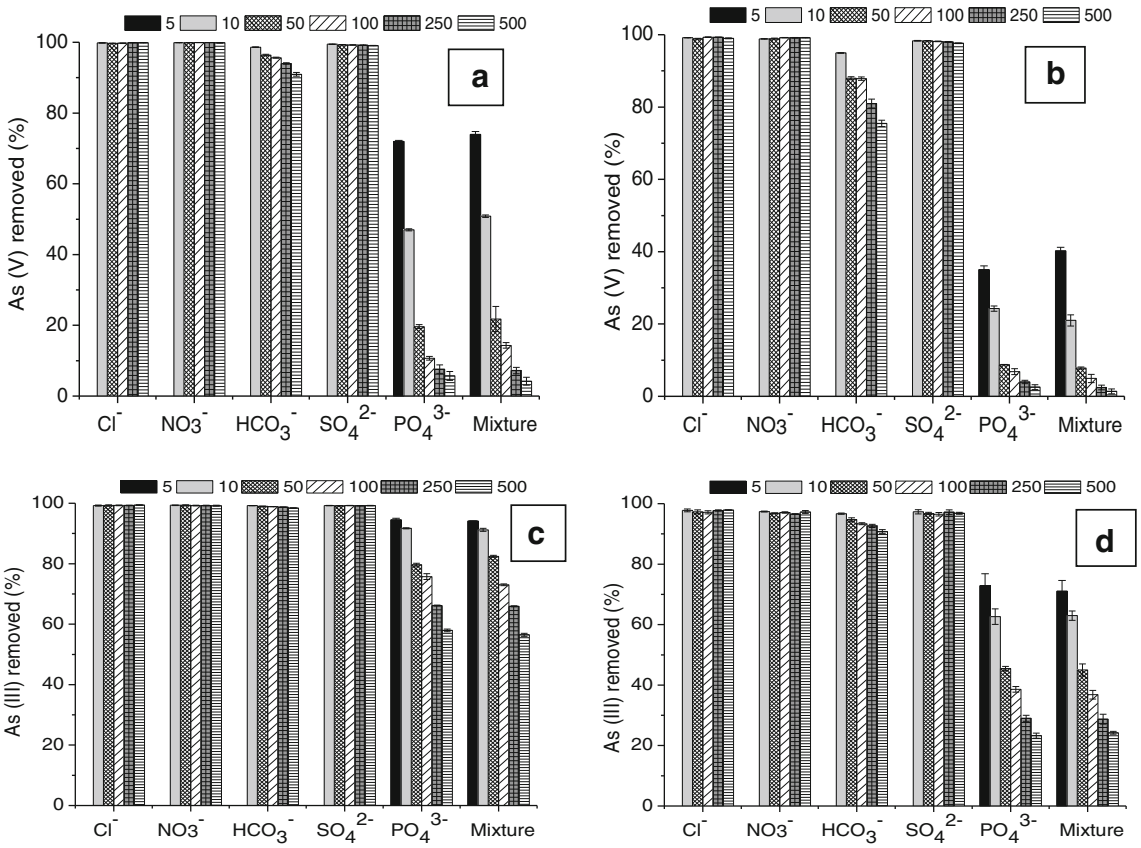

Fig. 8 Effect of co-existing anions on As(V) removal by **a** Ce-Pu (5-g/L dose) and **b** Ce-Rs (6-g/L dose) and As(III) removal by **c** Ce-Pu (5-g/L dose) and **d** Ce-Rs (6-g/L dose): initial As(III) or As(V) concentration was 0.25 mg/L, pH 7, shaking at 200 rpm for 2 h, at 24 ± 1 °C

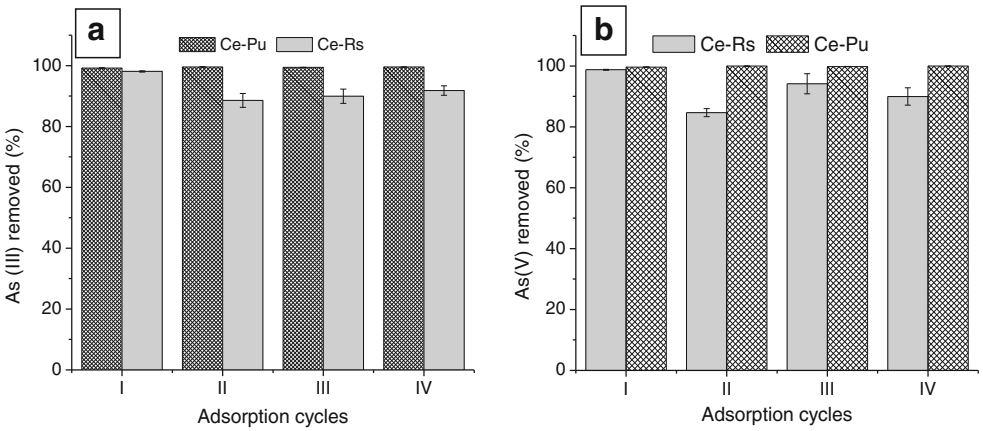

Fig. 9 Arsenic removal in subsequent adsorption cycles following desorption, using Ce-Pu and Ce-Rs as adsorbent. **a** As(III). **b** As(V)

energy of sorption, defined as the energy required to transfer one mole of ions to the surface of the solid from infinity in the solution (Boyaci et al. 2010). The E_{DR} value of an adsorption system is used to predict the mechanism of the adsorption process of a solute on a solid adsorbent. If the E_{DR} value is between 0 and 8 KJ/mol, the adsorption process is physical, whereas it is chemical if the E_{DR} is between 8 and 16 KJ/mol (Fufa et al. 2013). The values of E_{DR} computed for the equilibrium adsorption of As(III) on Ce-Pu and Ce-Rs were 13.2 and 14.2 kJ/mol, respectively. Similarly, for As(V) adsorption on Ce-Pu and Ce-Rs, the values were 17.2 and 18.3 kJ/mol, respectively. Similar results were also reported in previous studies (Alemu et al. 2014; D'Arcy et al. 2011). The adsorption energy (>8 kJ/mol) obtained in this study implies that the removal of As(III) and As(V) by Ce-Pu and Ce-Rs is dominated by chemisorption.

Effect of interfering anions

Experiments were conducted to understand the effect of increasing concentration of commonly occurring competitive anions on removal of As(III) and As(V) (Fig. 8a–d).

It is clear that Cl^-, NO_3^-, and SO_4^{2-} ions up to 500 mg/L concentrations have no significant effect on As(V) removal by both Ce-Pu and Ce-Rs, whereas HCO_3^- ions interfered slightly the adsorption of As(V). As the concentration of PO_4^{3-} increased from 5 to 500 mg/L, the As(V) removal potentials of the adsorbents reduced from 72 to 6% (Ce-Pu) and 35 to 3% (Ce-Rs). The removal efficiency of As(III) by Ce-Pu was not affected by Cl^-, NO_3^-, SO_4^{2-}, and HCO_3^- ions up to a concentration of 500 mg/L of each anion. However, the As(III) removal efficiency of Ce-Rs was slightly decreased in the presence of HCO_3^- ions. The presence of PO_4^{3-} also affected the removal of As(III) but the effect was less severe compared to As(V). The high adverse influence of phosphate on As(V) sorption than As(III) was also reported for many adsorbents (Basu and Ghosh 2013; Li et al. 2012). This is due to comparable size, charge, and structure of the PO_4^{3-} (aq) and AsO_4^{3-} (aq) oxyanions (Li et al. 2012), and therefore competition for similar sorption sites (Liu et al. 2001; Rouff et al. 2016). However, phosphate is absent or very rarely occurs at high concentrations in the groundwater, so its effect on As(III) and As(V) removal should not be a problem (Alemayehu 2004; McKenzie et al. 2001).

Reusability

Desorption experiments were carried out with the As(III)- or As(V)-loaded Ce-Pu and Ce-Rs using 0.1 M NaOH solution. The effect of recycling frequency on the adsorption performance of Ce-Pu and Ce-Rs was evaluated (Fig. 9). The removal efficiency of Ce-Pu and Ce-Rs was over 99 and 85%, respectively, after reusing it during four cycles, indicating that Ce-loaded volcanic rocks exhibited remarkable reusability.

Conclusion

Red scoria and pumice were successfully coated with cerium oxide using $Ce(NO_3)_3.6H_2O$. The produced Ce-Rs and Ce-Pu were used successfully to remove As(III) or As(V) from aqueous systems. A dose of 6 g/L of Ce-Rs or 5 g/L of Ce-Pu was found to be the optimum dose to lower arsenic concentrations of about 0.25 mg/L to a level below the WHO guideline. Both Ce-Rs and Ce-Pu showed high As(III) or As(V) removal efficiency in a pH range between 3 and 9, which is beneficial for real applications. The kinetics of As(III) and As(V) removal by the adsorbents were well expressed by pseudo-second-order model. The equilibrium data of As(III) and As(V) adsorption fitted better to the Freundlich and D-R models than the Langmuir isotherm. The D-R model predicts adsorption of As(III) or As(V) on Ce-Rs and Ce-Pu surfaces to be a chemisorption process. The Ce-loaded adsorbents can be recycled and used for removal of As(III) or As(V) up to four adsorption cycles without significant loss in efficiency. Accordingly, the batch adsorption experiment results suggest the suitability of

both Ce-Pu and Ce-Rs for removal of As(III) and As(V) from arsenic-contaminated water. Further study on simultaneous removal of As(III) and As(V) as well as evolution of the adsorbents efficiency using a real water sample of arsenic-affected areas, in batch and column modes, is required in order to scale up the process for real applications.

Acknowledgements The first author would like to thank Ghent University, Belgium, for the financial support through a Special Research Fund (BOF) fellowship. We are grateful to Elien Wallaert, Department of Materials Science and Engineering, Ghent University, Belgium, for the SEM and EDX measurements. The authors are also thankful to Tom Planckaert and Karen Leus, Department of Inorganic and Physical Chemistry, Ghent University, Belgium, for the BET analysis of the adsorbents.

References

Alemayehu T (2004) Water pollution by natural inorganic chemicals in the central part of the Main Ethiopian Rift. SINET: Ethiopian J Sci 23:197–214

Alemayehu E, Lennartz B (2009) Virgin volcanic rocks: kinetics and equilibrium studies for the adsorption of cadmium from water. J Hazard Mater 169:395–401

Alemu S, Mulugeta E, Zewge F, Chandravanshi BS (2014) Water defluoridation by aluminium oxide-manganese oxide composite material. Environ Technol 35:1893–1903

Appel C, Ma LQ, Rhue RD, Kennelley E (2003) Point of zero charge determination in soils and minerals via traditional methods and detection of electroacoustic mobility. Geoderma 113:77–93

Asere TG, De Clercq J, Verbeken K, Tessema DA, Fufa F, Stevens CV, Du Laing G (2017) Uptake of arsenate by aluminum (hydr)oxide coated red scoria and pumice. Appl Geochem 78:83–95

Asgari G, Roshani B, Ghanizadeh G (2012) The investigation of kinetic and isotherm of fluoride adsorption onto functionalize pumice stone. J Hazard Mater 217–218:123–132

Basu T, Ghosh UC (2013) Nano-structured iron (III)–cerium (IV) mixed oxide: synthesis, characterization and arsenic sorption kinetics in the presence of co-existing ions aiming to apply for high arsenic groundwater treatment. Appl Surf Sci 283:471–481

Biswas BK, Inoue K, Ghimire KN, Kawakita H, Ohto K, Harada H (2008) Effective removal of arsenic with lanthanum(III)- and cerium(III)-loaded orange waste gels. Sep Sci Technol 43:2144–2165

Bolt HM (2012) Arsenic: an ancient toxicant of continuous public health impact, from Iceman Otzi until now. Arch Toxicol 86:825–830

Boyaci E, Eroglu AE, Shahwan T (2010) Sorption of As(V) from waters using chitosan and chitosan-immobilized sodium silicate prior to atomic spectrometric determination. Talanta 80:1452–1460

Chen CJ, Chen CW, Wu MM, Kuo TL (1992) Cancer potential in liver, lung, bladder and kidney due to ingested inorganic arsenic in drinking water. Br J Cancer 66:888–892

Chiou H-Y, Hsueh Y-M, Liaw K-F, Horng S-F, Chiang M-H, Pu Y-S, Lin JS-N, Huang C-H, Chen C-J (1995) Incidence of internal cancers and ingested inorganic arsenic: a seven-year follow-up study in Taiwan. Cancer Res 55:1296–1300

D'Arcy M, Weiss D, Bluck M, Vilar R (2011) Adsorption kinetics, capacity and mechanism of arsenate and phosphate on a bifunctional TiO_2–Fe_2O_3 bi-composite. J Colloid Interface Sci 364:205–212

Elizalde-Gonzalez MP, Mattusch J, Einicke WD, Wennrich R (2001) Sorption on natural solids for arsenic removal. Chem Eng J 81: 187–195

Elson CM, Davies DH, Hayes ER (1980) Removal of arsenic from contaminated drinking-water by a chitosan-chitin mixture. Water Res 14:1307–1311

Far LB, Souri B, Heidari M, Khoshnavazi R (2012) Evaluation of iron and manganese-coated pumice application for the removal of As(V) from aqueous solutions. Iran J Environ Health Sci Eng 9:1

Fox DI, Stebbins DM, Alcantar NA (2016) Combining ferric salt and cactus mucilage for arsenic removal from water. Environ Sci Technol 50:2507–2513

Fufa F, Alemayehu E, Lennartz B (2013) Defluoridation of groundwater using termite mound. Water Air Soil Pollut 224:1552

Fufa F, Alemayehu E, Lennartz B (2014) Sorptive removal of arsenate using termite mound. J Environ Manag 132:188–196

Genz A, Kornmuller A, Jekel M (2004) Advanced phosphorus removal from membrane filtrates by adsorption on activated aluminium oxide and granulated ferric hydroxide. Water Res 38:3523–3530

Gupta K, Ghosh UC (2009) Arsenic removal using hydrous nanostructure iron(III)–titanium(IV) binary mixed oxide from aqueous solution. J Hazard Mater 161:884–892

Gupta VK, Saini VK, Jain N (2005) Adsorption of As(III) from aqueous solutions by iron oxide-coated sand. J Colloid Interface Sci 288:55–60

Guzman A, Nava JL, Coreno O, Rodriguez I, Gutierrez S (2016) Arsenic and fluoride removal from groundwater by electrocoagulation using a continuous filter-press reactor. Chemosphere 144:2113–2120

Haron MJ, Ab Rahim F, Abdullah AH, Hussein MZ, Kassim A (2008a) Sorption removal of arsenic by cerium-exchanged zeolite P. Mater Sci Eng B Adv Funct Solid State Mater 149:204–208

Haron MJ, Ab Rahim F, Abdullah AH, Hussein MZ, Kassim A (2008b) Sorption removal of arsenic by cerium-exchanged zeolite P. Mater Sci Eng B 149:204–208

He ZL, Tian SL, Ning P (2012) Adsorption of arsenate and arsenite from aqueous solutions by cerium-loaded cation exchange resin. J Rare Earths 30:563–572

He SF, Han CY, Wang H, Zhu WJ, He SY, He DD, Luo YM (2015) Uptake of arsenic(V) using alumina functionalized highly ordered mesoporous SBA-15 (Al-x-SBA-15) as an effective adsorbent. J Chem Eng Data 60:1300–1310

Heidari M, Moattar F, Naseri S, Samadi MT, Khorasani N (2011) Evaluation of aluminum-coated pumice as a potential arsenic(V) adsorbent from water resources. Int J Environ Res 5:447–456

Hsu JC, Lin CJ, Liao CH, Chen ST (2008) Removal of As(V) and As(III) by reclaimed iron-oxide coated sands. J Hazard Mater 153:817–826

Jadhav SV, Bringas E, Yadav GD, Rathod VK, Ortiz I, Marathe KV (2015) Arsenic and fluoride contaminated groundwaters: a review of current technologies for contaminants removal. J Environ Manag 162:306–325

Karimaian KA, Amrane A, Kazemian H, Panahi R, Zarrabi M (2013) Retention of phosphorous ions on natural and engineered waste pumice: characterization, equilibrium, competing ions, regeneration, kinetic, equilibrium and thermodynamic study. Appl Surf Sci 284:419–431

Kitchin KT, Wallace K (2005) Arsenite binding to synthetic peptides based on the Zn finger region and the estrogen binding region of the human estrogen receptor-α. Toxicol Appl Pharmacol 206:66–72

Kitis M, Kaplan SS, Karakaya E, Yigit NO, Civelekoglu G (2007) Adsorption of natural organic matter from waters by iron coated pumice. Chemosphere 66:130–138

Kumar KV (2006) Linear and non-linear regression analysis for the sorption kinetics of methylene blue onto activated carbon. J Hazard Mater 137:1538–1544

Kumar PS, Flores RQ, Sjostedt C, Onnby L (2016) Arsenic adsorption by iron-aluminium hydroxide coated onto macroporous supports: insights from X-ray absorption spectroscopy and comparison with granular ferric hydroxides. J Hazard Mater 302:166–174

Kundu S, Gupta AK (2006) Arsenic adsorption onto iron oxide-coated cement (IOCC): regression analysis of equilibrium data with several isotherm models and their optimization. Chem Eng J 122:93–106

Lakshmipathiraj P, Narasimhan BRV, Prabhakar S, Raju GB (2006) Adsorption studies of arsenic on Mn-substituted iron oxyhydroxide. J Colloid Interface Sci 304:317–322

Li Z, Qu J, Li H, Lim TC, Liu C (2011) Effect of cerium valence on As(V) adsorption by cerium-doped titanium dioxide adsorbents. Chem Eng J 175:207–212

Li R, Li Q, Gao S, Shang JK (2012) Exceptional arsenic adsorption performance of hydrous cerium oxide nanoparticles: part A. Adsorpt Capacit Mech Chem Eng J 185:127–135

Liu C, Evett J (2003) Soil properties—testing, Measurement, and Evaluation. Banta Book Company, USA ISBN 0-13-093005-9

Liu F, De Cristofaro A, Violante A (2001) Effect of pH, phosphate and oxalate on the adsorption/desorption of arsenate on/from goethite. Soil Sci 166:197–208

Liu B, Wang D, Yu G, Meng X (2013) Removal of F- from aqueous solution using Zr(IV) impregnated dithiocarbamate modified chitosan beads. Chem Eng J 228:224–231

Massoudinejad M, Asadi A, Vosoughi M, Gholami M, Karami MA (2015) A comprehensive study (kinetic, thermodynamic and equilibrium) of arsenic (V) adsorption using $KMnO_4$ modified clinoptilolite. Korean J Chem Eng 32:2078–2086

McKenzie JM, Siegel DI, Patterson W, McKenzie DJ (2001) A geochemical survey of spring water from the main Ethiopian rift valley, southern Ethiopia: implications for well-head protection. Hydrogeol J 9: 265–272

Mohapatra D, Mishra D, Chaudhury GR, Das RP (2007) Arsenic(V) adsorption mechanism using kaolinite, montmorillonite and illite from aqueous medium. J Environ Sci Health A-Toxic/Hazard Subst Environ Eng 42:463–469

Peric J, Trgo M, Medvidovic NV (2004) Removal of zinc, copper and lead by natural zeolite—a comparison of adsorption isotherms. Water Res 38:1893–1899

Pillewan P, Mukherjee S, Meher AK, Rayalu S, Bansiwal A (2014) Removal of arsenic (III) and arsenic (V) using copper exchange zeolite-a. Environ Prog Sustain Energy 33:1274–1282

Rijith S, Anirudhan TS, Sumi VSN, Shripathi T (2016) Sorptive potential of glutaraldehyde cross-linked epoxyaminated chitosan for the removal of Pb(II) from aqueous media: kinetics and thermodynamic profile. Desalin Water Treat 57:15083–15097

Rouff AA, Ma N, Kustka AB (2016) Adsorption of arsenic with struvite and hydroxylapatite in phosphate bearing solutions. Chemosphere 146:574–581

Sanchez-Cantu M, Galicia-Aguilar JA, Santamaria-Juarez D, Hernandez-Moreno LE (2016) Evaluation of the mixed oxides produced from hydrotalcite-like compound's thermal treatment in arsenic uptake. Appl Clay Sci 121:146–153

Sekomo CB, Rousseau DPL, Lens PNL (2012) Use of Gisenyi volcanic rock for adsorptive removal of Cd(II), Cu(II), Pb(II), and Zn(II) from wastewater. Water Air Soil Pollut 223:533–547

Sepehr MN, Zarrabi M, Kazemian H, Amrane A, Yaghmaian K, Ghaffari HR (2013) Removal of hardness agents, calcium and magnesium, by natural and alkaline modified pumice stones in single and binary systems. Appl Surf Sci 274:295–305

Sepehr MN, Amrane A, Karimaian KA, Zarrabi M, Ghaffari HR (2014) Potential of waste pumice and surface modified pumice for hexavalent chromium removal: characterization, equilibrium, thermodynamic and kinetic study. J Taiwan Inst Chem Eng 45:635–647

Sharma R, Singh N, Gupta A, Tiwari S, Tiwari SK, Dhakate SR (2014) Electrospun chitosan-polyvinyl alcohol composite nanofibers loaded with cerium for efficient removal of arsenic from contaminated water. J Mater Chem A 2:16669–16677

Singh TS, Pant KK (2004) Equilibrium, kinetics and thermodynamic studies for adsorption of As(III) on activated alumina. Sep Purif Technol 36:139–147

Singh R, Singh S, Parihar P, Singh VP, Prasad SM (2015) Arsenic contamination, consequences and remediation techniques: a review. Ecotoxicol Environ Saf 112:247–270

Styblo M, Del Razo LM, Vega L, Germolec DR, LeCluyse EL, Hamilton GA, Reed W, Wang C, Cullen WR, Thomas DJ (2000) Comparative toxicity of trivalent and pentavalent inorganic and methylated arsenicals in rat and human cells. Arch Toxicol 74:289–299

Tokunaga S, Wasay SA, Park S-W (1997) Removal of arsenic(V) ion from aqueous solutions by lanthanum compounds. Water Sci Technol 35:71–78

Viswanathan N, Sairam Sundaram C, Meenakshi S (2009) Development of multifunctional chitosan beads for fluoride removal. J Hazard Mater 167:325–331

Wang YX, Duan JM, Li W, Beecham S, Mulcahy D (2016) Aqueous arsenite removal by simultaneous ultraviolet photocatalytic oxidation-coagulation of titanium sulfate. J Hazard Mater 303:162–170

WHO (2006) Guidelines for drinking-water quality—first addendum to third edition, vol 1. WHO Press, Switzerland ISBN 92, 154696

Xie LY, Liu P, Zheng ZY, Weng SX, Huang JH (2016) Morphology engineering of V_2O_5/TiO_2 nanocomposites with enhanced visible light-driven photofunctions for arsenic removal. Appl Catal B Environ 184:347–354

Yazdani M, Tuudjarvi T, Bhatnagar A, Vahala R (2016) Adsorptive removal of arsenic(V) from aqueous phase by feldspars: kinetics, mechanism, and thermodynamic aspects of adsorption. J Mol Liq 214:149–156

Zhang Y, Yang M, Huang X (2003) Arsenic(V) removal with a Ce(IV)-doped iron oxide adsorbent. Chemosphere 51:945–952

Zhang Y, Dou XM, Zhao B, Yang M, Takayama T, Kato S (2010) Removal of arsenic by a granular Fe-Ce oxide adsorbent: fabrication conditions and performance. Chem Eng J 162:164–170

Zhong LS, Hu JS, Cao AM, Liu Q, Song WG, Wan LJ (2007) 3D flower-like ceria micro/nanocomposite structure and its application for water treatment and CO removal. Chem Mater 19:1648–1655